JOURNAL OF SPACECRAFT AND ROCKETS
Vol. 37, No. 1, January–February 2000

Mars Missions Using Solar Electric Propulsion

Steven N. Williams*
Jet Propulsion Laboratory, California Institute of Technology, Pasadena, California 91109
and
Victoria Coverstone-Carroll†
University of Illinois at Urbana–Champaign, Urbana, Illinois 61801

Successful demonstration of solar electric propulsion on the Deep Space 1 technology demonstration mission has paved the way for the use of this technology on future planetary missions. Currently there is much interest in retrieving Mars surface samples for scientific exploration, as well as developing the technology to enable human missions to Mars sometime in the next few decades. Solar electric propulsion trajectories for Mars opportunities in the 2004–2011 time frame are examined. All of the trajectories shown were optimized with a gradient based calculus-of-variations tool. In addition, a genetic algorithm was used to search for more nonstandard trajectories. Mission performance is presented as burnout mass along contours of constant flight time. The superior specific impulse of these propulsion systems results in a larger delivered mass at Mars than a conventional chemical mission. A very curious feature of these missions is that for longer flight times solutions exist that permit a nearly continuous launch opportunity over an entire Earth–Mars synodic period.

Nomenclature

C_3 = vis-viva energy ($V_p^2 - 2\mu/R_p$)
P = input to power processing unit
R_p = spacecraft periapsis radius
V_p = spacecraft periapsis velocity
V_∞ = hyperbolic excess velocity
μ = product of the universal gravitational constant and mass of central body

Introduction

THE possibility of discovering life elsewhere in the solar system has intrigued people for many decades. The announcement that evidence of life may have been found inside Martian meteorites has drawn further attention to this question. NASA is currently studying the possibility of retrieving several samples from the surface of Mars between 2005 and 2011. Without a doubt these will be the most ambitious planetary missions ever undertaken. As this paper is being written, mission planners want to deliver a lander to Mars in 2003 on a Delta III class launch vehicle and both an orbiter and lander in 2005 on an Ariane V. The landers will explore different locations on Mars. Each vehicle will carry a rover that will retrieve samples and an ascent vehicle that will deliver a sample back into Mars orbit. The orbiter will rendezvous separately with each of the ascent vehicles, transfer the samples, and return them to Earth. There will be many challenging aspects to these missions, not the least of which will be overcoming the large mass performance requirements on a streamlined budget.

We will show that there is a significant performance advantage to using solar electric propulsion (SEP) for Mars missions. We examine only the interplanetary phase of these missions. We do not consider Mars orbit insertion, or try to compare the various strategies one might use: chemical, aerobraking, aerocapture, SEP, or some combination of these. Also, the reader should recognize that the dry mass of a SEP system will be greater than that of a chemical system. This will consume some of the performance advantage shown later. Nevertheless, this performance advantage will be somewhere between 150 and 900 kg, depending on how one does the comparison, so that this should be sufficient to justify a serious examination of SEP for these missions.

We have previously compared SEP and chemical performance for several different planetary missions.[1] We believe a Mars sample return is an excellent example of the type of mission where SEP should be superior to conventional missions: a large interplanetary ΔV requirement on a mission that stays in the inner solar system. SEP is currently being tested on NASA's Deep Space 1 mission (DS1).[2] The successful demonstration of SEP on this mission should pave the way for its use on missions like the ones described in this paper.

In addition to Mars sample return missions, we also consider a less ambitious Mars orbiter mission. The interplanetary trajectories are computed in the same way. However, for the orbiter mission we assume a smaller launch vehicle and a simpler flight system. We show here that as the flight time is increased the launch period gets broader. At some point, as total mission flight time increases, we observe the rather curious fact that in most cases one can launch any day of the year with only small changes in mass performance. This behavior was initially discovered while examining a new technique (a hybrid genetic algorithm and calculus-of-variations approach) for low-thrust trajectory optimization.[3,4]

Models

The SEP trajectories reported in this paper were optimized with the Solar Electric Propulsion Trajectory Optimization Program (SEPTOP). SEPTOP is a modification of the Variable Thrust Trajectory Optimization Program (VARITOP).[5] The most important difference between the two programs is the more accurate model of the SEP performance characteristics found in SEPTOP. SEPTOP models the SEP throttling characteristics as a function of available solar array power. SEPTOP (and VARITOP) uses a traditional calculus-of-variations approach. SEPTOP computes an optimum trajectory such that the burnout mass is maximized by varying the thrust profile and launch energy (C_3). Injected mass at Earth is determined from a launch vehicle performance curve (holding a 5% contingency). A Delta II class launch vehicle (1300 kg injected mass to a C_3 of 0) was assumed for the orbiter missions and a Delta III class launch vehicle (2720 kg injected mass to a C_3 of 0) for the sample return missions. As just mentioned, no Mars orbit insertion strategy is considered. All SEP trajectories reported here rendezvous (match position and velocity) with Mars, that is, they arrive with a hyperbolic excess velocity (V_∞) of zero. A two-body gravitation model is used.

For SEP the key spacecraft parameters are thruster performance and solar array power. We assume NSTAR (NASA Solar

Received 5 March 1999; revision received 20 September 1999; accepted for publication 21 September 1999.

*Senior Engineer, Navigation and Flight Mechanics Section; Steven.N.Williams@jpl.nasa.gov. Member AIAA.
†Associate Professor, Department of Aeronautical and Astronautical Engineering; vcc@uiuc.edu. Senior Member AIAA.

Electric Propulsion Technology Applications Readiness Program) thrusters.[6] A polynomial approximation to thrust and mass flow rate was used:

$$\text{mass flow rate (mg/s)} = 0.74343 + 0.20951P + 0.25205P^2$$

$$\text{thrust (mN)} = -3.4318 + 37.365P \quad (1)$$

Maximum input power to each power processing unit (PPU) is 2.53 kW. Performance curves for the solar array were reported by Williams and Coverstone-Carroll.[1] Note that throughout the paper solar array power levels always represent the power generated at one astronomical unit (average distance of Earth from sun). SEP thrust and mass flow rate were reduced to 90% of their nominal value (referred to here as duty cycle) to provide additional margin and also account for time to perform optical navigation and other spacecraft functions incompatible with simultaneously operating the thrusters. For the orbiter missions one thruster and a 5-kW array were used. For the sample return trajectories two thrusters with 8- and 10-kW arrays were considered. In all cases 400 W of power were allocated to operate spacecraft systems and therefore not available to the SEP system.

Most of the results presented were found by performing parametric studies with SEPTOP. This involved following each of the contours shown (constant flight time) in the figures by incrementing the launch date and reoptimizing the trajectory. The algorithm in SEPTOP makes use of gradient information and in general works very well. Sometimes, when a fundamentally different solution becomes more optimum, the software has problems making the transition between the two. Frequently this implies a different sequence of thrust and coast phases.

We have been experimenting with optimization methods that do not rely entirely on gradients. One such successful experimentation coupled a multiobjective genetic algorithm with SEPTOP in hopes that by using the genetic algorithm's strength of evolving multiple solutions a large percentage of the search space could be sampled, and different classes of trajectories might be identified. The genetic algorithm was used to identify the initial values for the independent variables required to execute SEPTOP. This hybrid algorithm (genetic algorithm + SEPTOP) is described in detail by Hartmann et al.[3,4] The hybrid algorithm was applied to both the sample return and orbiter missions. In addition to identifying different classes of solutions, this technique also generates a set of trajectories within each class with similar characteristics—not unlike the parametric data generated with SEPTOP that will be discussed in this paper. As just stated, we did find a unique class of solutions using the hybrid algorithm, one of which is shown in Fig. 1. This particular solution consists of a series of four coast and four burn arcs. Because of the highly nonlinear nature of the SEPTOP independent variables (Lagrange multipliers), this solution would generally be quite challenging to find using SEPTOP as a stand-alone optimizer. Typically, once one solution is found other similar solutions can be obtained by changing some parameter (launch or encounter dates, flight time, etc.) and reoptimizing the trajectory. This approach generally works well, but is not 100% reliable. In fact, having found the solution (in Fig. 1) with the hybrid software, we tried unsuccessfully to transition between it and the other solutions we found using the parametric techniques just described. There apparently are barriers or steep gradients in one or more of the independent variables that will not permit a gradient-based algorithm to make the transition.

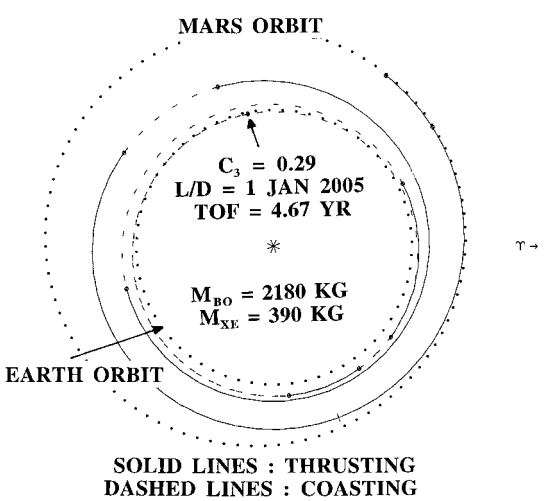

Fig. 1 Long flight time Mars trajectory.

Sample Return Missions

We computed trajectories to Mars for launch dates between the middle of 2004 and late 2009, slightly less than three Earth–Mars synodic periods. The results are shown in Figs. 2a and 2b. This time span covers three distinct sets of opportunities. We show contours of constant flight time between 1.5 and 3.0 years. We used a 10-kW solar array to power two NSTAR thrusters. In Fig. 2b we provide more detail for the first opportunity than in Fig. 2a and also show the effect of less power (8 kW). All of the trajectories in these figures arrive at Mars with a V_∞ of 0.0. In practice, the method used for Mars orbit insertion might be chemical, SEP, or some form of aerocapture, but as already mentioned, this phase of the mission is not modeled. We also point out that SEP can be used to arrive with any desired V_∞. Figure 3 shows the performance impact of arriving at different velocities on a two-year mission launched in July 2005 (from Fig. 2b).

For comparison purposes we indicate the location of each ballistic or chemical opportunity with a vertical dashed line. We also provide performance results in Table 1 for several chemical orbit insertion strategies. The aerocapture cases simulate a situation where no propulsive energy is required for Mars orbit insertion. Comparing the "Burnout mass" column in Table 1 to Fig. 2, one immediately sees that the SEP will almost certainly outperform any strategy, which relies on a propulsive Mars capture. Nevertheless, the results presented here do not allow one to make a direct comparison, both because the SEP trajectories shown do not achieve a Mars capture orbit and because the difference between SEP and chemical propulsion system masses is not provided. Also, in addition to a full SEP scenario, one might want to examine SEP with an aerocapture strategy at Mars. We show in Fig. 3 that the SEP can be used to achieve any desired approach velocity. Nevertheless, the purpose of this paper is not to suggest that SEP is clearly the best option because many necessary trades remain to be done. We do believe, however, the results shown here indicate that SEP may provide a significant performance benefit for Mars missions and that further examination of this approach is warranted.

Figures 2a and 2b display the SEP results used to analyze the Earth to Mars portion of the sample return mission. The performance of the shorter flight time trajectories displays a familiar behavior with a single maximum, tapering off rapidly in a symmetrical manner as you move away from the optimum launch date. However, as the

Table 1 Chemical mission performance characteristics

Capture mode	L/D	C_3, km^2/s^2	TOF, yr	Burnout mass, kg[a]	Propellant mass, kg
Aerocapture[b]	1 Sept. 05[c]	15.45	1.101	1817	0
	22 Sept. 07[d]	12.75	1.011	1940	0
	14 Oct. 09[e]	10.27	0.897	2056	0
3-day Mars orbit[f]	4 Aug. 05	16.65	0.933	1299	465
	11 Sept. 07	13.57	0.939	1503	398
	13 Oct. 09	10.28	0.887	1636	420
1-day Mars orbit[f]	4 Aug. 05	16.65	0.933	1249	515
	11 Sept. 07	13.57	0.939	1446	456
	13 Oct. 09	10.28	0.887	1573	483
Low circular orbit[f]	4 Aug. 05	16.65	0.933	869	895
	11 Sept. 07	13.57	0.939	1006	896
	13 Oct. 09	10.28	0.887	1094	962

[a]Delta III class launch vehicle, Isp = 320 s.
[b]Launch/arrival dates optimized to minimize C_3 (arrival periapsis radius = 3900 km).
[c]Mars arrival V_∞ = 3.51 km/s.
[d]Mars arrival V_∞ = 2.83 km/s.
[e]Mars arrival V_∞ = 2.47 km/s.
[f]Launch/arrival dates optimized to minimize C_3 + arrival ΔV (arrival periapsis radius = 3900 km).

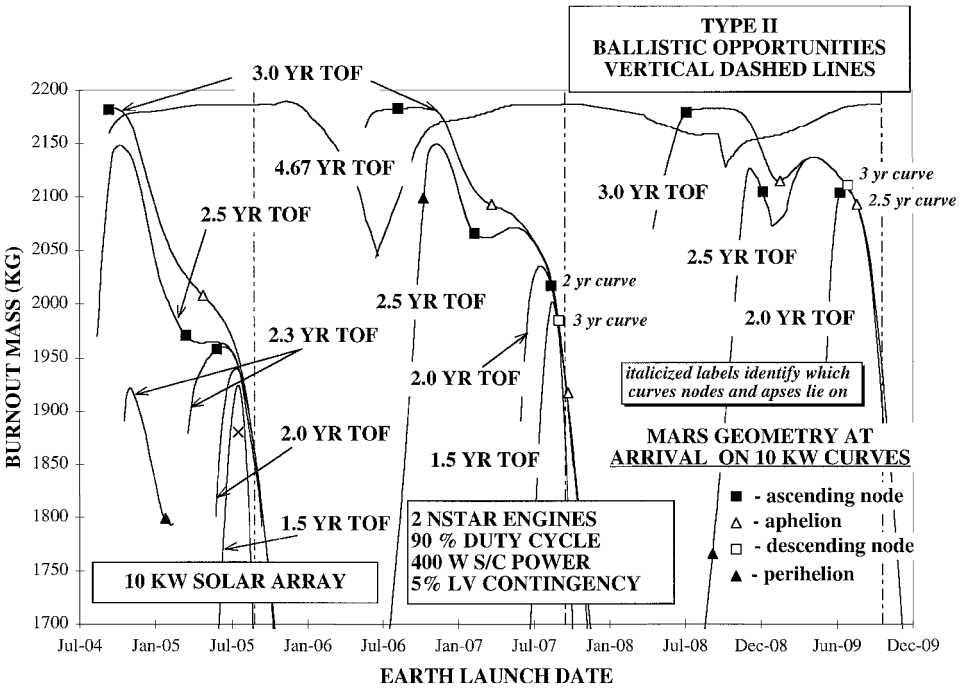

Fig. 2a SEP Earth-to-Mars mass performance (Delta III).

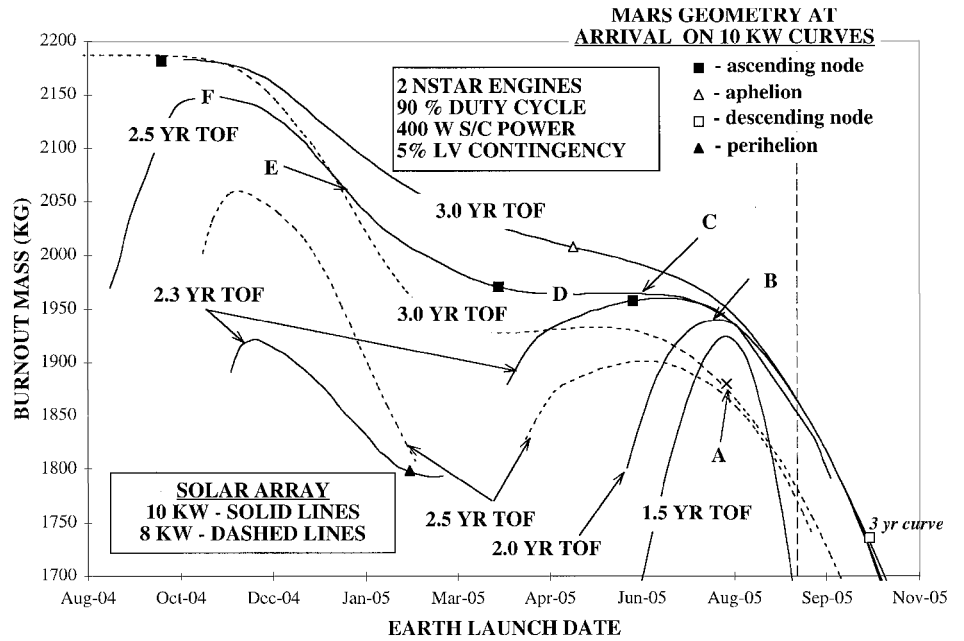

Fig. 2b 2005 SEP Earth-to-Mars mass performance.

flight time is increased, one observes a rather peculiar behavior. A second maximum appears with an earlier launch date. At first, there are two maxima, which are not continuously connected, but further increases in the flight time results in a continuous set of solutions between the two maxima. At longer flight times the later maxima transitions into an inflection point and eventually disappears so that only the earlier one is present. Finally, at even longer flight times (4.67 years here) there are continuous solutions across the entire 5.5 years shown in the plot.

As mentioned earlier, we could not transition between the two types of solutions (4.67 and 3.5 years) using SEPTOP alone. As just explained, these solutions are too different for a gradient technique to bridge the gap. In this case the long flight time will make the result impractical for Mars mission design purposes but can be important in understanding the sometimes nonintuitive nature of low-thrust trajectories. It also illustrates the fact that the traditional pure gradient-based methods for doing interplanetary trajectory optimization are fine for doing parametric studies over a region where only moderate changes are expected to occur. However, they will be inadequate when searching for SEP trajectories on many missions where a more complicated interplanetary trajectory (multiple heliocentric revolutions or multiple gravity-assist encounters or both) is required.

One might expect the best performance to correlate with arriving at Mars at a node (as with ballistic trajectories) so that the SEP does not have to thrust out of the ecliptic plane, or to arrive near perihelion where the power and therefore available thrust are the greatest. These points are shown on the curves in Figs. 2a and 2b. Interestingly, for the 1.5-year flight times, the optimum solution results in a compromise, which falls between these points. As one goes to longer flight times, the correlation is better. Both the 2- and 3-year flight times want to arrive near the ascending node. The

Table 2 Trajectory characteristics for selected missions

Trajectory type	L/D	C_3/declination of launch asymptote	Burnout mass, kg	Propellant mass, kg	Thrust sequence[a]	Heliocentric revolutions
A	4 Aug. 05	9.9/7.5	1880	196	b	0.81
B	26 July 05	7.9/10.7	1939	235	b–c–b	1.18
C	6 June 05	6.8/−10.3	1965	264	b–c–b–c–b	1.52
D	7 May 05	6.0/−22.5	1964	305	b–c–b–c–b	1.56
E	12 Jan. 05	2.9/7.6	2056	374	b–c–b	1.69
F	29 Oct. 04	1.9/28.5	2148	334	b–c–b–c–b	1.77

[a]b = burn or thrust arc and c = coast arc.

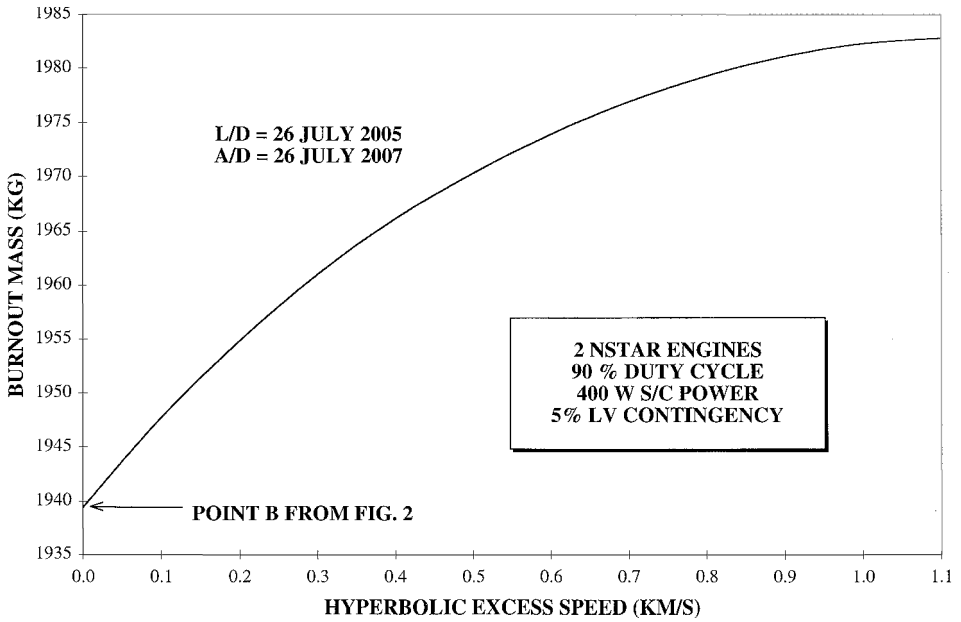

Fig. 3 SEP mass performance vs Mars arrival V_∞.

2.5-year curves are more like the 1.5-year curves, with the peak performance falling between these points.

It is also instructive to examine the change in the trajectory at selected points in Fig. 2b. The trajectories in Fig. 4 correspond to the letters A–F in Fig. 2b. Additional information on these trajectories is shown in Table 2. The letters C–F are all on the 2.5-year contour in Fig. 2b. The solutions at A and B represent other points of interest. The solution at A is the shortest flight time (1.4 year) in this family of solutions, which can be flown (subject to the other constraints in the problem: launch vehicle performance curve, solar array, duty cycle). It requires continuous unbroken thrusting from launch to Mars arrival. The trajectory at point B represents the peak performance on the 2-year curve and contains one coast arc. Point C represents a local optimum on the 2.5-year curve. Here the optimum solution now has a second coast arc. Point D represents a slight dip in the performance where the two coast arcs have shifted somewhat. At point E the second coast arc has disappeared leaving only one coast arc again. Finally at point F, which has the greater performance of the two optima, a second coast arc has appeared early in the mission. Point F is also unique in one other aspect. The others reach solar ranges near Mars very early in the mission. They then either fall back in or use the SEP to rendezvous with Mars as quickly as possible. The point F trajectory has a more continuous spiral out to Mars, doing more of its thrusting well inside Mars' orbit where the SEP is more effective. This results in better mass performance.

Consistent with the preceding discussion, one can see in Table 2 that increased performance (burnout mass) corresponds to decreasing launch energy. This is not too surprising because it means more of the mission ΔV is being imparted with the more efficient SEP than with the launch vehicle upper stage. In this example the increased performance also correlates with larger heliocentric revolutions. The best performance occurs when the planetary geometry is such that the transfer angle is greatest. This permits a lower C_3 (and therefore larger injected mass) and a tighter spiral, which means more time is spent close to the sun where the SEP is more effective. This can be seen in Eq. (1). Thrust is proportional to PPU input power, which decreases as the spacecraft moves away from the sun.

Figure 5 shows similar plots for Earth return trajectories. These trajectories all begin at Mars with a V_∞ of zero and an initial mass of 700 kg. For these trajectories the V_∞ at Earth is not part of the cost function. Propellant consumption is minimized, and the Earth arrival velocity is derived from the relative speed between Earth and spacecraft at arrival, without being a constraint in the problem as it is for the rendezvous trajectories discussed above. As in Fig. 2, there is also some indication of double maxima in these plots, although it varies somewhat from year to year. There is no evidence that a longer return time translates into better performance—just a broader opportunity. Also, the 10-kW array provides very little advantage over the 8-kW array for the return leg. The choice of 700 kg was somewhat arbitrary. A more realistic value would require a more detailed mass estimate for the spacecraft and Earth reentry vehicle, but this is probably a reasonable first approximation. As a point of reference, the DS1 inert spacecraft mass (including everything but xenon) with only one thruster and a 2.5-kW array was about 400 kg.

Figure 6 illustrates how the trajectory changes for four points from Fig. 5. Point A represents the maximum performance on the 1-year curve. It consists of a fairly simple profile with a burn arc followed by a coast arc. As the flight time is increased between A and B, the departure date moves earlier, but the beginning of the thrust arc stays about the same (to within a week). For all practical purposes A and B are the same trajectory. These trajectories arrive back at Earth with a V_∞ of about 2.65 km/s. Points C and D are local maxima on the 2-year curve. Between B and C an early thrust arc has appeared, and the original thrust arc has shortened in duration. Both are about three months long. The Earth V_∞ has also gone up.

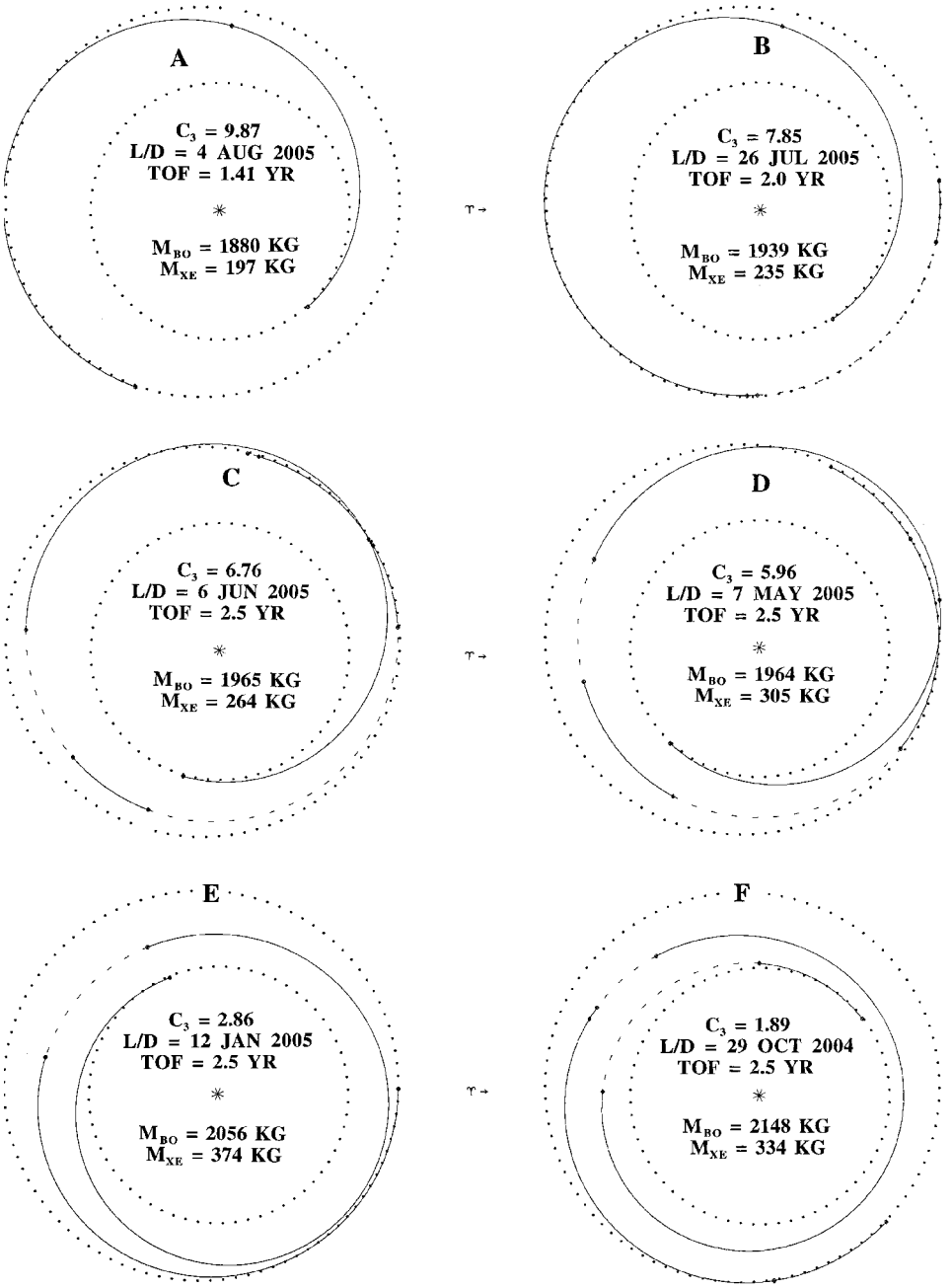

Fig. 4 SEP Earth-to-Mars heliocentric trajectory plots (2004–2005).

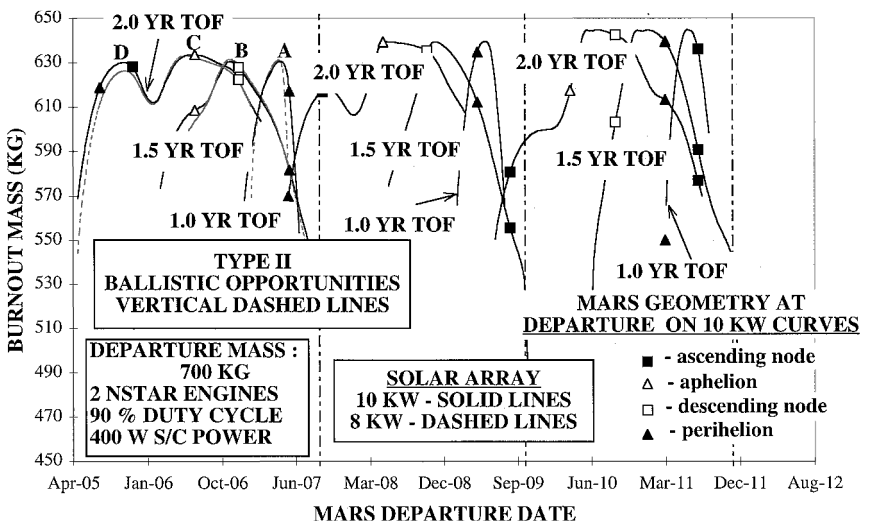

Fig. 5 SEP Mars-to-Earth mass performance.

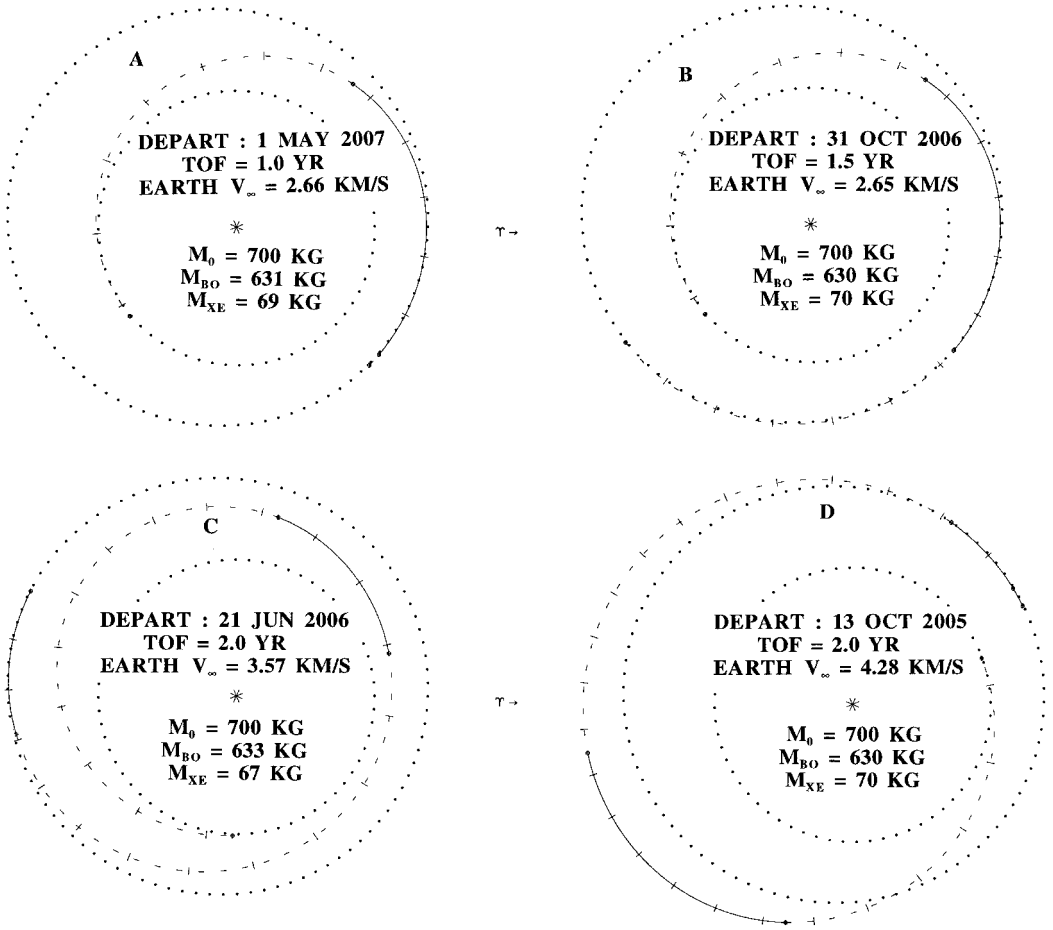

Fig. 6 SEP Mars-to-Earth heliocentric trajectory plots (2005–2007).

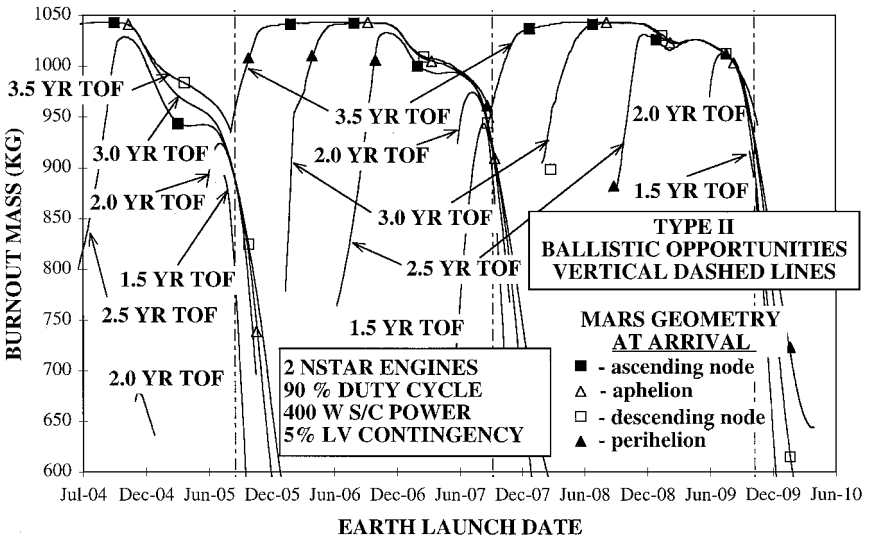

Fig. 7 SEP Earth-to-Mars mass performance (Delta II).

Although the effect is small here, similar to trajectory F in Fig. 4, note that C does a larger fraction of its thrusting closer to the sun (where the SEP is more effective) than the other three, and also has the better mass performance. In D the earlier thrust arc has increased in duration while the later one has shortened. It has slightly less mass performance than C.

Orbiter Missions

Trajectories to Mars for launch dates between the middle of 2004 and late 2009 were computed. The results are shown in Fig. 7. This time span covers three distinct sets of opportunities. We show contours of constant flight time between 1.5 and 3.5 years. For these trajectories we used a Delta II class launch vehicle and a 5-kW solar array to power the SEP. As in Fig. 2, these trajectories arrive at Mars with $V_\infty = 0$. In the 2005 opportunity we see behavior very similar to that in Fig. 2a with double maxima. The other two opportunities show some evidence of the double maxima, but look more like the profiles in Fig. 5 where longer flight times give broader launch opportunities, but not much performance advantage. As before, we indicate the location of each ballistic or chemical opportunity with

a vertical dashed line. Using the genetic algorithm code described earlier, we found a 3.5-year contour to be continuous across the range of launch dates examined.

Conclusions

We believe there are two important conclusions to be drawn from this analysis. The first is that SEP has the potential to offer significant performance advantage to Mars sample return missions currently being studied. Solar electric propulsion vs chemical propulsion systems is a trade that must be done on a mission-by-mission basis. However, missions with large ΔV requirements in the inner solar system can take advantage of the superior performance characteristics of ion propulsion and are precisely the type of mission where SEP should compare favorably with chemical systems. The Mars rendezvous and departure require a large interplanetary ΔV, and the mission remains in the inner solar system where solar power is available to drive the SEP.

We showed that for short flight times SEP performance curves have a symmetric profile similar to ballistic trajectories. As the flight time increases, the trajectories become more complicated with a series of burn-coast arcs, which result in somewhat nonintuitive behavior. We also showed that using SEP allows one to significantly reduce and also vary the arrival velocity, reducing the thermal load on an aerobrake or aerocapture mission if one were combined with the SEP.

The second conclusion is that in designing interplanetary SEP missions we are limited when using only traditional gradient-based optimization techniques. It would have been very difficult, if not impossible, to find the trajectories that exhibited the continuous launch opportunities using only the gradient-based software. Even with trajectories as simple as Earth to Mars, SEP can produce some surprising results, although in this case the continuous launch period solutions will probably have too long a flight time to be practical. The point is that for relatively simple (or moderately difficult) trajectories these traditional techniques work fine. If we ever want to fly SEP versions of multiple gravity-assist trajectories such as the Galileo or Cassini missions, we will almost certainly have to incorporate non-gradient-based techniques such as genetic algorithms to map the complete solution space.

Acknowledgment

The research described in this paper was carried out by the Jet Propulsion Laboratory, California Institute of Technology, under a contract with NASA.

References

[1]Williams, S. N., and Coverstone-Carroll, V., "Benefits of Solar Electric Propulsion for the Next Generation of Planetary Exploration Missions," *Journal of the Astronautical Sciences*, Vol. 45, No. 2, 1997, pp. 143–159.

[2]Rayman, M. D., Chadbourne, P. A., Culwell, J. S., and Williams, S. N., "Mission Design for Deep Space 1: A Low-Thrust Technology Validation Mission," International Academy of Astronautics, Paper L98-0502, April 1998.

[3]Hartmann, J. W., Coverstone-Carroll, V., and Williams, S. N., "Optimal Interplanetary Spacecraft Trajectories via a Pareto Genetic Algorithm," American Astronautical Society, Paper 98-202, Feb. 1998.

[4]Hartmann, J. W., Coverstone-Carroll, V., and Williams, S. N., "Optimal Interplanetary Spacecraft Trajectories via a Pareto Genetic Algorithm," *Journal of the Astronautical Sciences*, Vol. 46, No. 3, 1998, pp. 267–282.

[5]Sauer, C. G., Jr., "Optimization of Multiple Target Electric Propulsion Trajectories," AIAA Paper 73-205, Jan. 1973.

[6]Sovey, J. S., Hamley, J. A., Haag, T. W., Patterson, M. J., Pencil, E. J., Peterson, T. T., Pinero, L. R., Power, J. L., Rawlin, V. K., Sarmiento, C. J., Anderson, J. R., Becker, R. A., Brophy, J. R., Polk, J. E., Benson, G., Bond, T. A., Cardwell, G. I., Christensen, J. A., Freick, K. J., Hamel, D. J., Hart, S. L., McDowell, J., Norenberg, K. A., Phelps, T. K., Solis, E., Yost, H., and Matranga, M., "Development of an Ion Thruster and Power Processor for New Millennium's Deep Space 1 Mission," AIAA Paper 97-2778, July 1997; also NASA TM 113129, Dec. 1997.

J. A. Martin
Associate Editor